OPEN ACCESS

ACTA METALLURGICA SLOVACA

2026, VOL. 32, NO. 1, 15-20

RESEARCH PAPER

Study of the mechanism of vanadium sorption on anion-exchange resin

Nazigul Zhumakynbay, Nazira Seidakhmetova, Bagzhan Ondiris, Abylaikhan Akhmetov*

RSE National Centre on Complex Processing of Mineral Raw Materials of the Republic of Kazakhstan, Zhandosova Street, No. 67, 050036 Almaty, Almaty Province, Kazakhstan

*Corresponding author: erkej@mail.ru, tel.: +7 778 203 4223, RSE National Centre on Complex Processing of Mineral Raw Materials of the Republic of Kazakhstan, Zhandosova Street, No. 67, 050036 Almaty, Almaty Province, Kazakhstan

Received: 24.11.2025
Accepted: 08.12.2025

ABSTRACT

This article presents the results of a study of the mechanism of vanadium sorption from productive solutions of black shale ores using the macroporous, strongly basic anion-exchange resin Biolite 200U. The studies were conducted at pH 1.5–1.9, where vanadium is predominantly present as anionic compounds (meta-, poly-, and decavanadates). Using IR spectroscopy and X-ray diffraction analysis, it was established that the sorption process involves the exchange of vanadate ions with the quaternary ammonium centres of the resin and is accompanied by the participation of bridging sulfate groups. The formation of stable complex compounds with the precipitation of Na_3VO_4 and $VOCl_3$ phases was detected. Based on the data obtained, a mechanism for the sorption of vanadium in the form of stable phase compounds is proposed.

Keywords: black shales, sorption, vanadate complexes, bidentate bond, IR spectroscopy, X-ray phase analysis

INTRODUCTION

Vanadium is a rare but strategically important metal with high industrial potential and a wide range of applications. According to global analytical agencies [1,2], total vanadium reserves amount to approximately 38 million tons, with the largest resources concentrated in China, Russia, and South Africa, which determines the market's geographic specificity and issues of raw material security.

The largest volume of vanadium consumption occurs in metallurgy, where it is used as an effective alloying element in the production of steels and alloys, providing increased strength, wear resistance, and corrosion resistance [3]. Vanadium is of significant importance in aviation, space, and nuclear technology, where materials with high heat resistance and stability under extreme operating conditions are required [4]. A separate area of application involves the use of vanadium in catalysts for the petrochemical and chemical industries, as well as in pharmaceuticals, ceramics, glass, and the creation of vanadium redox batteries (VRFB), a promising energy storage technology for renewable energy sources [5].

Vanadium is primarily extracted from titanomagnetites (0.05–0.8% V) and phosphorus iron ores (0.03–0.1% V). Vanadium is extracted from these ores as a by-product in the form of vanadium oxides (V_2O_5, V_2O_3), which are then processed into ferrovanadium or nitrided vanadium for alloying [6–9].

The continued growth in demand for vanadium, given the limited supply of high-quality ores, is driving the need to integrate not only traditional sources but also off-balance-sheet and man-made sources into processing. These include metallurgical slags, coal combustion ash, low-grade titanomagnetites, and black shale formations. Their use is considered one of the most promising areas for securing a vanadium resource base, which requires the development of effective technologies for its extraction and concentration.

Kazakhstan possesses some of the world's largest vanadium reserves, with the main source being the black shale rocks of the Greater Karatau, which account for approximately 70% of the resource, making them strategically important for industrial development [10]. The vanadium content of black shales ranges from 0.2 to 0.6% by V, making this resource considered off-balance.

Vanadium occurs in natural and man-made sources in four oxidation states (V(II), V(III), V(IV), V(V)) as oxides, silicates, phosphates, and complex silicates with iron, aluminum, calcium, and magnesium. These ore types are primarily processed using hydrometallurgical methods, which are characterized by low selectivity, high impurity levels, and depend on the acidity and redox potential of the solutions [11, 12]. Sorption methods ensure the selective extraction of anionic vanadium forms, thereby reducing the content of associated impurities, and exhibit high cyclic stability during sorption, desorption, and resin regeneration [13-15].

The basis of the black shale ore processing process is autoclave leaching [16-19]. The resulting productive solution under these conditions is characterized by a multi-component, complex composition. Along with vanadium, the solution contains many impurity metals—iron, phosphorus, aluminum, sodium, potassium, uranium, etc.

The ionic state of vanadium as a function of pH is shown in **Fig. 1** [20,21].

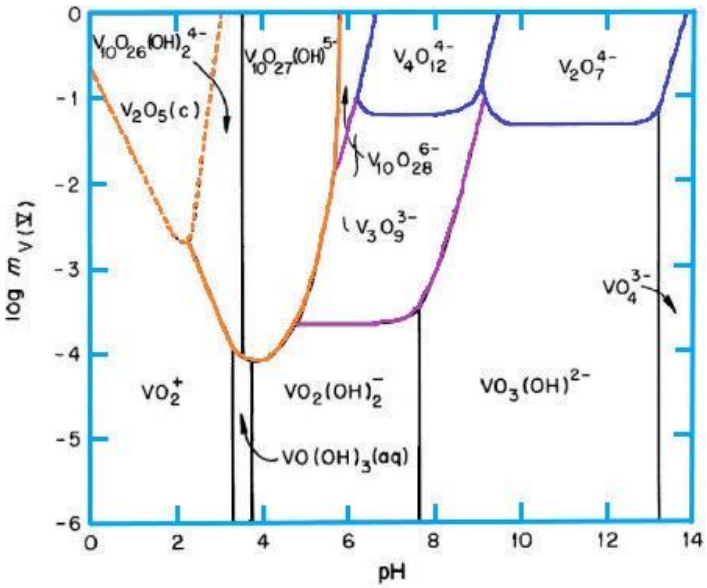

Fig. 1 Different regions of existence of vanadate ions depending on pH

Previously, strongly basic anion exchangers VP-1p, VP-1Ap, AM, AM-p, AMP, and ampholytes such as ANKB were used for vanadium sorption from industrial solutions over the pH range 1-8. Sorbents AM-p and ANKB have the highest capacity, with the anion exchanger AM-p having the best kinetic characteristics. Equilibrium during vanadium sorption by this ion exchanger is achieved in 5 hours, while for sorbents VP-1p and VP-1Ap this time is 24 hours. However, the listed advantages turn into disadvantages as soon as it comes to sorbent

regeneration. High capacities and wide pH ranges of sorption require the use of concentrated acid and alkali solutions for desorption [22, 23]. In [24], studies were conducted using the following sorbents: Ambersep 920, AM-p, Purolite 3848, Lewatit 600, and Amberlite 910. The results showed that Ambersep 920 was the most effective sorbent. These sorbents exhibit mechanical strength during resin desorption and regeneration.

One such new type is the anion exchange resin Biolite 200U. This sorbent is used in uranium mining enterprises. Biolite 200U exhibits selectivity for uranyl sulfate complexes. Unlike traditional anion exchange resins available on the market, Biolite 200U is significantly less expensive, which is noteworthy. In addition to the uranium industry, it is also promising for extracting rare and non-ferrous metals from industrial solutions.

This study aims to investigate the mechanism of vanadium sorption on the anion-exchange resin Biolite 200U, determine the features of the interaction of vanadate complexes with the sorbent's functional groups, and assess the influence of this process on the efficiency of extraction of the target component.

MATERIAL AND METHODS

The sorption solution was obtained by autoclave leaching black shale ore from the Balasauskandyk deposit. The characteristics of the productive solution are presented in **Table 1**.

Table 1 Characteristics of the productive solution

Components	V_2O_5	UO_3	MoO_3	ΣРЗЭO_3	P_2O_5	Fe^{3+}/Fe^{2+}	Al_2O_3	ORP, mV	pH
Content, g/dm^3	3,5-3,7	0,0045	0,0075	0,30	2,4	7,5	6,3	+450 -490	1,1-1,2

The characteristics of the anion exchange resin Biolite 200U are presented in **Table 2** in comparison with Ambersep 920.

Sorption was carried out in a static mode: stirring was performed in beakers at a resin:solution volume ratio of 30:900 Vcm:Vp, at 50°C, and for 12 hours. Experiments were conducted at pH 1.5 and 1.9.

The degree of vanadium extraction is calculated depending on the metal concentration in the solution. The pH and ORP of aqueous solutions are measured with an I-500 pH meter equipped with a built-in platinum electrode.

The chemical composition of the material was determined using PANalytical (currently Malvern Panalytical) software and an X-ray fluorescence (XRF) spectrometer. The mention of "Pressed powder" and calibration confirmed that the analysis was carried out via energy-dispersive or wavelength-dispersive XRF (EDXRF or WDXRF).

X-ray diffraction analysis (XRD): X-ray diffraction (XRD) was performed on a D8 Advance (Bruker) instrument, using α-Cu at 40 kV and 40 mA. Diffraction data were processed, and interplanar spacings were calculated using DIFFRAC.EVA software. Sample decryption and phase identification were performed using the Search/Match program using the PDF-2 Powder Diffraction Database, release 2023.

Spectra were obtained on an FT/IR-6X (JASCO, Japan) Fourier transform IR spectrometer in the 4000-400 cm-1 spectral range from 50 mg tablets prepared by pressing after dilution with KBr 2:100. The KBr spectrum was used as a reference. Spectra Manager Ver.2.5 software was used. Spectra analysis was performed using specialized literature.

Table 2 Comparative table of the physical and chemical characteristics of the ion exchange resins Ambersep 920 and Biolite 200U

Indicator	Standard / Method	Test Results	
		Ambersep 920	SQD201U
Type of ion-exchange resin	Type of ion-exchange resin	Type of ion-exchange resin	Type of ion-exchange resin
Functional groups		Tertiary amine (R_3N)	Quaternary ammonium (R_4N^+)
Ionic form as supplied		Chloride form	Chloride form
Physical form	GOST 10900-84	Spherical granules	Spherical granules
Bulk density, g/cm³	GOST 10898.2-74	0,55	0,68
Moisture content, %	GOST 1 0898.1 -84	48,79	51,34
Specific volume, cm³/g	GOST 10898.4-84	2,89	3,01
Swelling coefficient	GOST 10898.4-84	1,45	1,7
Mechanical strength at drum rotation speed 200 rpm, %		97	98
Chemical stability and mechanical strength under operational condition changes, %		92	94
Granulometric composition (by wet sieving method, %)			
+2,0		0,0	0,0
-2,0+1,8		0,0	0,0
-1,8+1,6		0,0	0,0
-1,6+1,4		0,0	0,0
-1,4+1,25		0,0	0,0
-1,25+1,0		0,0	53,0
-1,0+0,8		0,0	46,0
-0,8+0,63		6,5	1,0
-0,63+0,5		70,5	0,0
-0,5+0,4		23,0	0,0
Stability: Temperature range PH range		from 1 to 70^{0}C from 0 to 14	from 1 to 85^{0}C from 0 to 14

RESULTS AND DISCUSSION

In vanadium chemistry, sorption, ion-exchange resin saturation, and impurity content primarily depend on the medium's pH. Vanadium sorption occurs within a pH range of 4.0-1.5. A pH below the boundary zone leads to the formation of vanadium cations in solution that are not sorbed by the anion exchange resin and can also increase impurities in the anion exchange resin. An upper pH limit of 4.5 reduces sorption capacity due to the formation of supramolecular vanadium complexes. These data confirm previous studies on vanadium sorption on AM-p and Ambersep 920 anion exchange resins, which reported an optimal pH range of 1.5-1.9 [25-27].

Based on the sorption results, the chemical analysis of the sorbents during sorption is presented in **Table 3**.

Table 3 Chemical Analysis of Saturated Sorbents

Compound formula	Concentration of metals at pH sorption 1,5 (%)	Concentration of metals at pH sorption 1,9 (%)
O	13,071	13,253
Na	0,496	0,937
Mg	0,023	0,028
Al	0,259	0,427
Si	0,104	0,142
P	0,531	0,622
S	12,468	12,914
Cl	3,199	2,480
K	0,055	0,085
Ca	0,191	0,117
Ti	0,376	0,629
V	3,373	3,175
Cr	0,112	Not revealed
Fe	4,567	7,354
Cu	0,048	0,071
Se	0,009	0,019
Mo	0,153	0,209
U	0,255	0,320
Ni	Not revealed	0,024
As	Not revealed	0,019

Chemical analysis after sorption on the sorbent revealed the presence of numerous impurities in addition to vanadium.

We conducted an IR spectroscopic analysis of the original Biolite 200U anion exchange resin. The resulting curves (**Fig. 2**) reveal characteristic bands in the IR spectrum of the anion exchange resin corresponding to the functional groups of its organic matrix. The band at 3401 cm^{-1} corresponds to the stretching vibrations of OH groups in water, indicating the presence of adsorbed moisture. The peaks at 3020 cm^{-1} and 2924 cm^{-1} correspond to the stretching vibrations of the aromatic C–H and CH_2 groups, confirming the styrene matrix structure of the quaternary amine. In the region of 1614–1488 cm^{-1}, bands of C=C stretching vibrations of the aromatic ring are observed; the band at 1222 cm^{-1} is associated with C–N stretching vibrations of amines, which indicates the presence of functional ammonium groups. In-plane deformation vibrations of C–H of the disubstituted benzene ring appear at 976 and 925 cm^{-1}, and the band at 890 cm^{-1} corresponds to vibrations of quaternary ammonium groups $N^+(CH_3)_3$, confirming the cationic nature of the active centers of the sorbent. Out-of-plane deformation vibrations of C–H of the disubstituted benzene ring (859 and 828 cm^{-1}) and C–H of the monosubstituted benzene ring (706 cm^{-1}) are also recorded, reflecting the presence of incompletely converted polystyrene [28,29].

Thus, the spectrum confirms the structure of the anion exchange resin as a polystyrene material with quaternary ammonium functional groups.

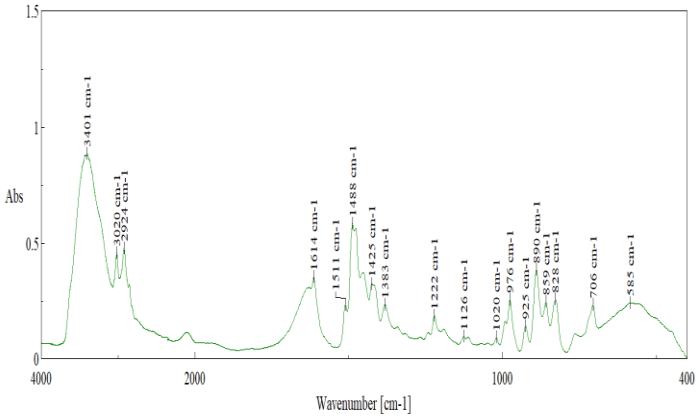

Fig. 2 Infrared spectrum of the original anion exchange resin Biolite 200U

The IR spectrum of the saturated Biolite 200U anion exchange resin (**Fig. 3**) at pH -1.5 displays absorption bands similar to those of the original anion exchange resin. A complex group of bands at 1173, 1107, and 1047 cm^{-1} has changed, corresponding to the asymmetric $\nu_3(SO_4^{2-})$ stretching mode. Their triple splitting indicates a decrease in sulfate anion symmetry from Td to C_{2v}, which is associated with the bidentate bridging of SO_4^{2-} on the resin's cationic centers. Signals near 976 cm^{-1} are due to ν(V=O) stretching vibrations of vanadyls and/or vanadates. Their overlap with the δ(C–H) in-plane deformation vibrations of disubstituted aromatic rings complicates direct identification. Nevertheless, the strengthening and broadening of this band after sorption indirectly indicate the presence of vanadium in the V(V) form. In the range of 890–828 cm^{-1}, out-of-plane deformations δ(C–H) of aromatic rings are observed, as well as a signal of trialkylammonium groups (approximately 890 cm^{-1}). Although it is in this region that bridging vibrations of V–O–V (900–700 cm^{-1}) are usually observed, the bands of the polymer matrix dominate, preventing us from isolating the specific signals of polyvanadates. The bands at 766 and 706 cm^{-1} are associated with out-of-plane deformations δ(C–H) of aromatic rings and indicate the preservation of the polystyrene backbone of the resin. Also, in the range of 665–583 cm^{-1}, a triple splitting of deformation vibrations $\nu_4(SO_4^{2-})$ is recorded. This effect also confirms the bridging bidentate coordination of sulfate anions at the active sites of the resin, resulting in a reduction in symmetry to C_{2v} [28,29].

Thus, the combined spectral data confirm the preservation of the polystyrene matrix of the resin and the fixation of sulfate anions in the bidentate form. Additional broadening of the peak at 976 cm^{-1} indicates the involvement of vanadium (V) in the sorption process in the form of vanadate complexes.

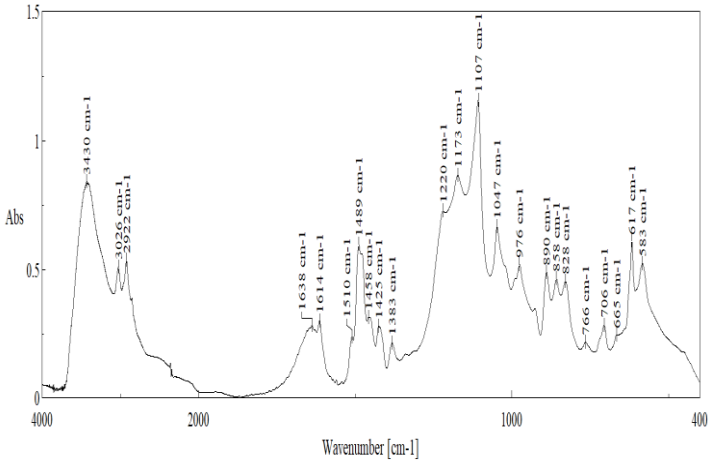

Fig. 3 Infrared spectrum of saturated anion exchange resin Biolite 200U at pH 1.5

Comparing the two spectra (the original anion exchange resin-black-versus the saturated anion exchange resin-blue-we can see that the blue spectrum clearly exhibits enhanced peaks in the 1200–1000 and 700–500 cm^{-1} ranges, indicating the formation of sulfate complexes (**Fig. 4**). This means that after sorption, SO_4^{2-} and vanadate ions are fixed to the resin, accompanied by a change in symmetry and enhanced bands.

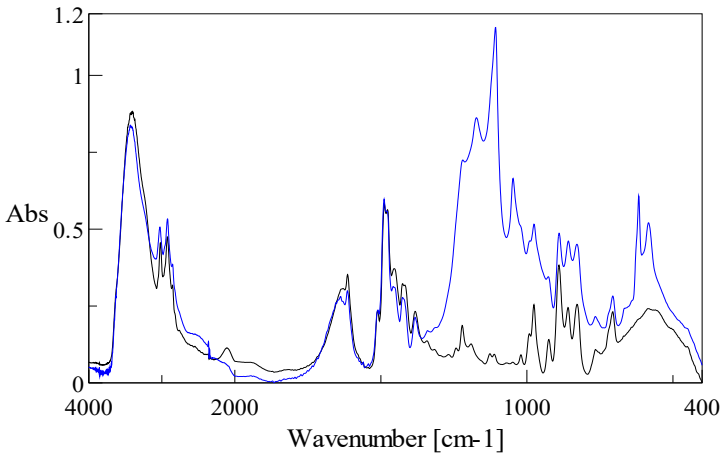

Fig. 4 Infrared spectrum of the original (black) and saturated 3 (blue) anion exchange resin Biolite 200U at pH 1.5

Literary sources [28,29] indicate that the bridging bidentate coordination of sulfate anions means that the sulfate ion is coordinated by two oxygen atoms to two different centers. This "bridge" configuration emphasizes that the sulfate is held by not one, but two bonds, which increases the strength of the bond. A vanadium complex (VO_3^- or VO_2^+) is added nearby, also coordinating at the same centers via an oxygen group. This creates a mixed complex in which sulfate and vanadate participate in bonding through joint coordination.
Vanadium is present in different phases within the anion exchanger, as shown in X-ray phase analysis (**Fig. 5**).

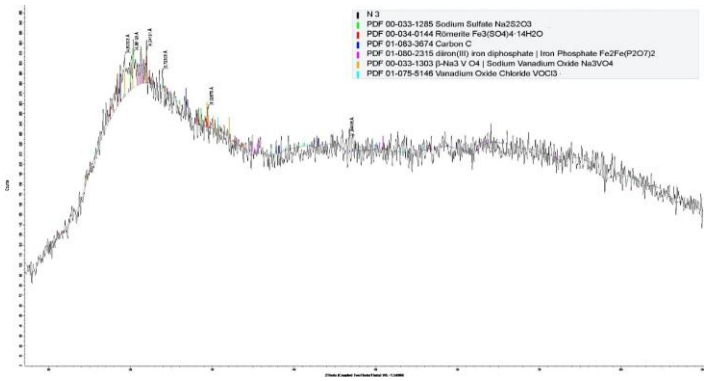

Fig. 5 X-ray phase analysis of saturated anion exchange resin Biolite 200U at pH 1.5

XRD analysis confirms the complex multicomponent structure of the sorbent after interaction with the model solution, including sulfate, phosphate, and vanadate phases. The main indicators of vanadium sorption are peaks corresponding to Na_3VO_4 and $VOCl_3$, which are consistent with IR spectroscopy data indicating the fixation of V(V) as vanadate complexes.
To confirm the previously obtained data, IR spectroscopic analysis of the saturated anion exchange resin Biolite 200U was also performed at pH 1.9 (**Fig. 6**). The spectrum, along with the sorbent absorption, displays absorption bands of the sulfate complex at 1170, 1109, 1047, 665, 617, and 584 cm-1. A splitting of the ν3 and ν4 vibrations into three components is observed (ν3 - 1170, 1109, 1047 cm-1 and ν4 - 665, 617, 584 cm-1), this indicates a decrease in the symmetry of the SO4 2- ion to C2υ, therefore, in this complex the SO4 2- group can be a bridging bidentate one [28, 29]. The appearance and strengthening of the band in the region of 976 cm^{-1}, as well as weak signals in the range of 900–700 cm^{-1}, indicate the fixation of vanadium mainly in the form of vanadate complexes V(V) with the possible formation of polyvanadate structures. Low-frequency vibrations in the region of 466–418 cm^{-1} indicate the formation of V–O type bonds.

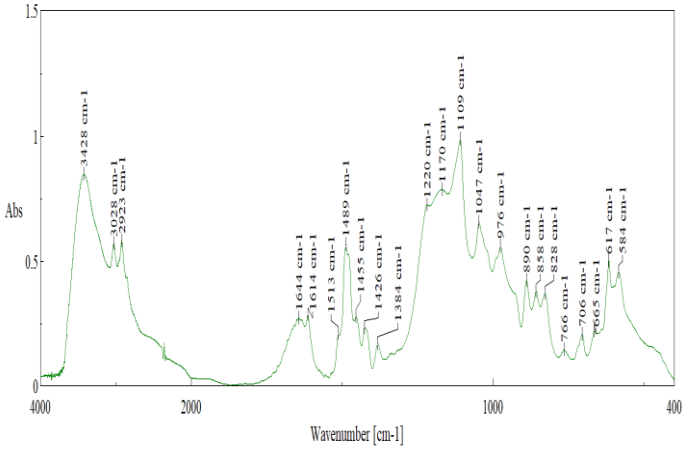

Fig. 6 Infrared spectrum of saturated anion exchange resin Biolite 200U at pH 1.9

Fig. 7 also compares the original spectrum (black curve) with the saturated spectrum at pH 1.9 (red line). More pronounced splitting confirms the reduction in the symmetry of SO_4^{2-} (from Td to C_{2v}) and their bidentate bridging anchoring on the active sites of the resin. A more intense band at 976 cm^{-1} appears in the spectrum after sorption, characteristic of the ν(V=O) stretching vibrations of the vanadyl and vanadate groups. This is a key indicator of the presence of vanadium in the V(V) form. Signals at 900–700 cm^{-1} in this region are associated with possible V–O–V bridging vibrations in polyvanadates. Superposition with the δ(C–H) deformation vibrations of the aromatic matrix complicates precise signal separation; however, the presence of additional shoulders confirms the formation of multidimensional vanadate structures. After sorption, signals at 600–400 cm^{-1} indicate enhanced low-frequency vibrations, suggesting the formation of V–O bonds and impurities, such as Fe–O, which participate in the formation of coordination complexes.

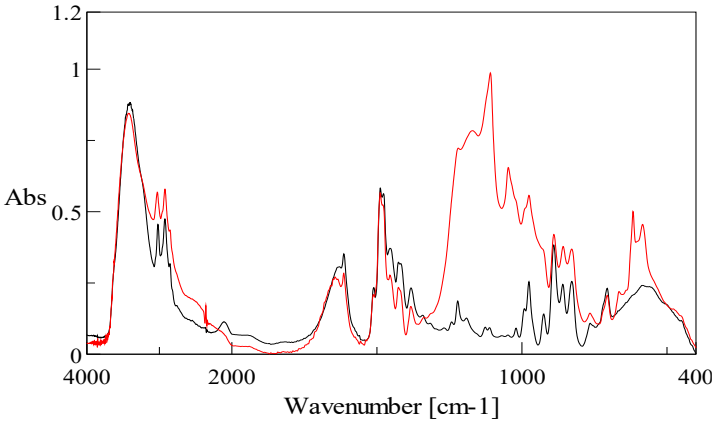

Fig. 7 Infrared spectrum of the original (black) and saturated 3(red) anion exchange resin Biolite 200U at pH 1.9

To visualise the changes across all three spectra, **Fig. 8** shows them. As shown in the spectrum, the red and blue lines are virtually identical, indicating a single sorption mechanism across pH values.

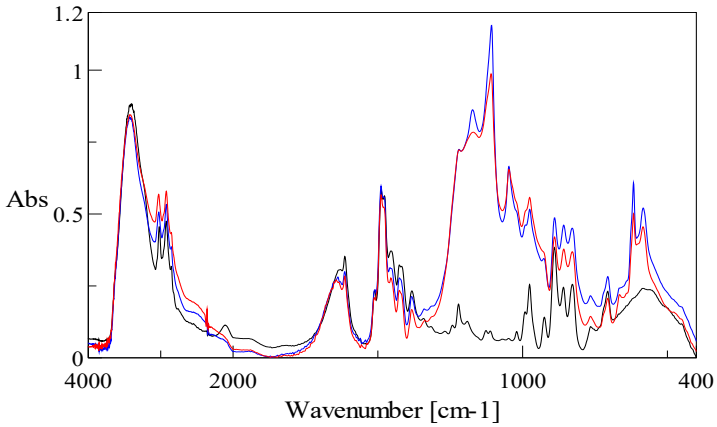

Fig. 8 Infrared spectrum of the original (black), saturated 3(red) anionite Biolite 200U at pH 1.5, saturated 3(red) anionite Biolite 200U at pH 1.9

The diffraction pattern of a saturated anion exchanger at pH 1.9 is shown in **Fig. 9**.

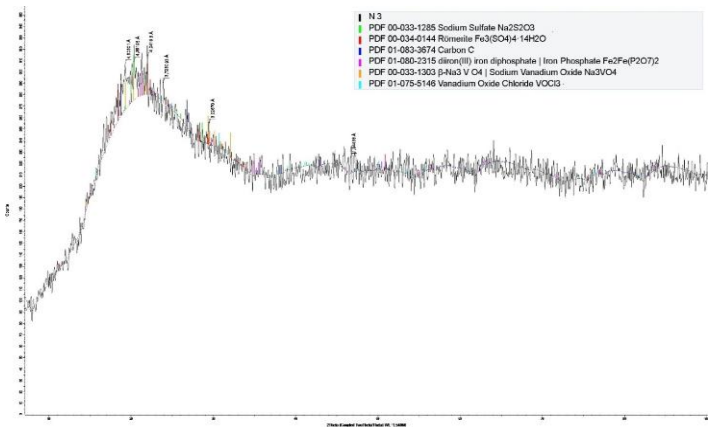

Fig. 9 X-ray phase analysis of saturated anion exchange resin Biolite 200U at pH 1.9

XRD analysis, similar to that for sorption at pH 1.5, confirms the complex multicomponent structure of the sorbent after interaction with the model solution, including sulfate, phosphate, and vanadate phases. Here, too, the main indicators of vanadium sorption are the peaks of Na_3VO_4 and $VOCl_3$, which is consistent with IR spectroscopy data indicating the fixation of V(V) as vanadate complexes.

CONCLUSION

This study experimentally demonstrates the high potential of the strongly basic macroporous anion-exchange resin Biolite 200U for extracting vanadium from productive solutions of black shale ores. Sorption experiments were conducted at pH 1.5–1.9, where vanadium is present primarily in the form of anionic complexes (meta-, poly-, and decavanadates). IR spectroscopy showed that the initial anion exchange resin contains a polystyrene matrix and quaternary ammonium functional groups. The IR spectra of the saturated resins show virtually identical curves, according to which the amplification and splitting of the ν_3 and ν_4 SO_4^{2-} bands indicate bridging bidentate coordination of the sulfate anions. The strengthening of the band at 976 cm^{-1} and additional signals in the 900–700 cm^{-1} region confirm the fixation of vanadium in the form of vanadate and polyvanadate complexes of V(V). Low-frequency vibrations (466–418 cm^{-1}) are associated with V–O bond formation, indicating strong vanadium fixation at the active sites. X-ray phase analysis revealed the multicomponent composition of the saturated resins: $Na_2S_2O_3$, Römerite $Fe_3(SO_4)_4$ $14H_2O$, $Fe_2Fe(P_2O_7)_2$, Na_3VO_4, $VOCl_3$, and others. The presence of Na_3VO_4 and $VOCl_3$ phases confirms the fixation of vanadium in the resin structure as vanadate compounds, consistent with IR spectroscopy results.

Thus, the studies suggest the following mechanism for vanadium sorption on Biolite 200U:

- ion exchange between the quaternary ammonium groups of the resin and vanadate anions;
- joint coordination of sulfate and vanadate ions as bridging complexes;
- the formation of stable vanadate phases (Na_3VO_4, $VOCl_3$) within the sorbent structure.

Overall, it has been established that Biolite 200U is an effective sorbent for extracting vanadium from complex multicomponent solutions, ensuring selective binding of vanadate forms of V(V) and the formation of stable coordination complexes.

Acknowledgements: This research has been funded by the Science Committee of the Ministry of Science and Higher Education of the Republic of Kazakhstan (Grant No. AP19578967).

REFERENCES

1. U.S. Geological Survey. Vanadium: Mineral Commodity Summary 2025. https://pubs.usgs.gov/periodicals/mcs2025/mcs2025-vanadium.pdf?utm_source (accepted 20/09/2025)
2. *Vesting News Network. "Top 4 Vanadium-producing Countries."* (2025) https://investingnews.com/daily/resource-investing/battery-metals-investing/vanadium-investing/vanadium-producing-countries/?utm_source (accepted 20/09/2025)
3. I.A. Ditenberg, I.V. Smirnov, K.V. Grinyaev, A.N. Tyumentsev, V.M. Chernov, M.M. Potapenko, S.A. Kulinich: Materials, 16(6), 2023, 2430. https://doi.org/10.3390/ma16062430
4. Muroga, T. (2012). Vanadium for nuclear systems. In Comprehensive Nuclear Materials (Vol. 4, pp. 411–434). Elsevier. https://doi.org/10.1016/B978-0-08-056033-5.00094-X
5. E.B. Agyekum, M. Abdullah, F. Odoi-Yorke, A. Ameen, P. Chowdhury, M.A. Raza, F.L. Rashid, A.K. Hussein: Energy Conversion and Management, 27, 2025, 101180. https://doi.org/10.1016/j.ecmx.2025.101180
6. G.N. Nazarov, Zh.K. Akhmetov: *Geochemistry of black shale strata of Karatau.* Almaty: Nauka, 1992.
7. V.D. Fedorov, A.M. Chekmaryov: Geologiya Nefti i Gaza, (8), 1986, 35–42.
8. B.P. Tissot, D.H. Welte: *Petroleum Formation and Occurrence.* Berlin: Springer, 1984.
9. Kiseleva Yu.A., Zheglova T.P., Dakhnova M.V., Mozhegova S.V., Nazarova E.S., Nechitailo G.S. (2017). The role of Domanik deposits in the formation of oil pools in the central areas of the Volga–Ural petroleum province (Buzuluk depression). *Russ. Geol. Geophys. (2017) 58 (3-4): 310–321.*https://doi.org/10.1016/j.rgg.2016.09.007
10. Rychkov V.N., et al.: Hydrometallurgy, 175, 2018, 55–63. https://doi.org/10.1016/j.hydromet.2017.11.004
11. Zhu, X.; Yang, X.; Ma, C.; Li, W. Journal of Water Process Engineering, 2023, 104380. https://doi.org/10.1016/j.jwpe.2023.104380
12. T. Zhang, T. Liu, Y. Zhang, H. Liu: Batteries, 9(5), 2023, 240. https://doi.org/10.3390/batteries9050240
13. Yu C., Bao Sh., Zhang Y. Separation and adsorption of V(V) from vanadium-containing solution by TOMAC-impregnated resins, 2021. Chemical Engineering Research and Design 174(11–12), https://doi.org/10.1016/j.cherd.2021.08.019
14. A.R. Chakhmouradian, M.P. Smith: Ore Geology Reviews, 131, 2021, 103983. https://doi.org/10.1016/j.oregeorev.2021.103983
15. C. Li, W. Li, H. Huang, J. Chen, Y. Zhang: ACS Omega, 9(19), 2024, 17352–17361. https://doi.org/10.1021/acsomega.4c01417
16. V.A. Kozlov, N.M. Komokova, G.Zh. Zhunusova, N. Zhumakynbai: Research Journal of Pharmaceutical, Biological and Chemical Sciences, 7(2), 2016, 1973–1982.
17. N.M. Komekova, V.A. Kozlov, K.M. Smirnov, R.A. Shayakhmetova, K.N. Nesterov: Metallurgist, 60(11–12), 2017, 1186–1190. https://doi.org/10.1007/s11015-017-0427-7

18. N.M. Komekova, V.A. Kozlov, R.A. Shayakhmetova, G.R. Saisanova: Industry of Kazakhstan, 2, 2015, 16–18.
19. E.N. Zholdybaev, I.O. Aimbetova, V.A. Kozlov, S.B. Nurzhanova, A.A. Zharmenov: *Method of processing vanadium-containing ores*. Patent KZ 24105. Publ. 25.12.2012.
20. N.I. Gumerova, A. Rompel: Chemical Society Reviews, 49, 2020, 7568-7601. https://doi.org/10.1039/D0CS00392A
21. M. Aureliano, N.I. Gumerova, G. Sciortino, E. Garribba, A. Rompel, D.C. Crans: Coordination Chemistry Reviews, 2021, 447, 214143. https://doi.org/10.1016/j.ccr.2021.214143
22. E.N. Suleimenov, V.A. Kozlov, L.A. Bimendina, E.A. Bekturov: *Self-organization of organic and inorganic polymers in water*. Gylym: Almaty, 1999.
23. A.S. Goncharenko: *Electrochemistry of vanadium and its compounds*. Moscow: Metallurgy, 1969.
24. V.A. Kozlov, L.Kh. Batrakova, S.B. Nurzhanova, Ya.V. Grazhdanova: Modern problems of vanadium metallogeny in oils, *Proceedings of the scientific and practical conference Metallogeny of individual metals (noble, rare, non-ferrous and other metals)*, Tashkent, p. 90–92, 2002.
25. A. Wołowicz, Z. Hubicki: Molecules, 27(17), 2022, 5432. https://doi.org/10.3390/molecules27175432
26. V.A. Kozlov, et al.: *Method for processing vanadium-containing raw materials*, Patent of the Russian Federation No. 2374344, Published 27.11.2009.
27. N.D. Bridzhen, et al.: *Method of autoclave processing of black shale ores*, Patent RK 26644, published 25.12.2012.
28. B.N. Laskorin: *Ion-exchange materials for hydrometallurgical processes*, wastewater treatment and water preparation: Handbook, Moscow: VNIIKhT, 1983.
29. K. Nakamoto: *IR and Raman spectra of inorganic and coordination compounds*, Translated from English, Moscow: Mir, 1991.